Journal of Membrane Science 389 (2012) 205–215

Contents lists available at SciVerse ScienceDirect

Journal of Membrane Science

journal homepage: www.elsevier.com/locate/memsci

Ca-containing CO_2-tolerant perovskite materials for oxygen separation

Konstantin Efimov*, Tobias Klande, Nadine Juditzki, Armin Feldhoff

Institute of Physical Chemistry and Electrochemistry, Leibniz Universität, Hannover, Callinstraße 3-3A, D-30167 Hannover, Germany

ARTICLE INFO

Article history:
Received 3 June 2011
Received in revised form 3 September 2011
Accepted 22 October 2011
Available online 29 October 2011

Keywords:
Mixed ionic-electronic conductor
Perovskite, CO_2-stability
Asymmetric membrane
In-situ X-ray diffraction
Transmission electron microscopy

ABSTRACT

Perovskites $(La_{1-x}Ca_x)FeO_{3-\delta}$ and $(La_{1-x}Ca_x)(Co_{0.8}Fe_{0.2})O_{3-\delta}$ with varying La and Ca contents ($x = 0.4$–0.6) were designed by sol–gel route as model membrane materials to be an alternative to Ba- and Sr-based systems for operation in the presence of CO_2. It was found that only the first members of the systems with $x = 0.4$ consisted of almost pure perovskite phases. The materials containing more Ca ($x = 0.5$–0.6) exhibited a considerable amount of bi-phase material, such as brownmillerite and/or spinel, after calcination at 1223 K. The orthorhombicly distorted $(La_{0.6}Ca_{0.4})FeO_{3-\delta}$ and rhombohedrally distorted $(La_{0.6}Ca_{0.4})(Co_{0.8}Fe_{0.2})O_{3-\delta}$ perovskites showed relatively high oxygen permeation fluxes at 1223 K of 0.26 $cm^3\,min^{-1}\,cm^{-2}$ and 0.43 $cm^3\,min^{-1}\,cm^{-2}$, respectively. The oxygen-ionic conductivity of the materials was improved by about 50% via an asymmetric configuration using a porous support and an approximately 10-μm thick dense layer with the same chemical composition. *In situ* XRD in an atmosphere containing 50 vol.% CO_2 and long-term oxygen permeation experiments using pure CO_2 as the sweep gas revealed a high tolerance of Ca-based materials toward CO_2. Thus, we suggest that Ca-containing perovskite can be considered promising membrane materials if operation in the presence of CO_2 is required.

1. Introduction

Over the last two decades, mixed oxygen ionic and electronic conductors (MIECs) have attracted a lot of attention. Because of their very high oxygen-ionic transport rates over a wide temperature range, the Ba- and Sr-containing perovskites [e.g., $(Ba_{1-x}Sr_x)(Co_{0.8}Fe_{0.2})O_{3-\delta}$ and $(La_{1-x}Sr_x)(Co_{1-y}Fe_y)O_{3-\delta}$] rank among the state-of-the-art MIEC materials [1–3]. However, the wide practical employment of these materials is hindered by significant problems, like poor chemical and thermomechanical stability [4–10]. In particular, the degradation of these materials in the presence of CO_2, with the formation of carbonates, [11–16] handicaps their application in important processes, such as cathode materials in solid-oxide fuel cells (SOFCs) operated at intermediate temperatures, in oxyfuel processes or in hydrocarbon partial oxidations, where some CO_2 is formed as a bi-product of an undesired deeper oxidation [17–19].

Tolerance against CO_2 can be achieved by the complete replacement of Ba and Sr in the A lattice site of the perovskite structure by rare-earth elements, like La. Unfortunately, this leads to a dramatic loss in the oxygen-ionic conductivity of the materials, as caused by a reduced lattice parameter, which induces lower oxygen mobility, and by a lower amount of mobile oxygen vacancies, which results from a higher oxidation state of the rare-earth cation [20]. To increase the oxygen deficiency in the perovskite lattice, a Ca cation with the stable valence state of 2+ can be regarded as a potential dopant.

The stability of alkaline earth-containing materials in the presence of CO_2 can be evaluated using the Ellingham diagram shown in Fig. 1. This figure demonstrates the thermodynamic stability of carbonates at a given CO_2 partial pressure and temperature. The compact lines with positive slope in the diagram represent chemical potentials of CO_2 during the decomposition of corresponding carbonate, which is equal to negative value of free enthalpy of decomposition reaction, as calculated with thermodynamic data using free enthalpy of formation of corresponding educts and products or determined experimentally [21–24]. The dashed lines give the chemical potential of CO_2 at different partial pressures. In general, if the CO_2 chemical potential of the carbonate decomposition reaction at the present temperature is higher than at the corresponding partial pressure, the carbonates are thermodynamically unstable. As can be seen in the Ellingham diagram, $CaCO_3$ is significantly less stable than $BaCO_3$ and $SrCO_3$. The relatively small ionic radius of 135 pm of the Ca^{2+} cation, as compared with Ba^{2+} ($r = 160$ pm) Sr^{2+} and ($r = 144$ pm) cations, leads to a decline of the crystal lattice energy of carbonate and can be considered a reason for the lower stability of $CaCO_3$ [25,26]. Note, the Ellingham diagram gives only a rough guide to estimate the possible tolerance of Ca-containing perovskite materials against CO_2 because the stabilization energy of perovskite may also play an important role

* Corresponding author. Tel.: +49 511 762 2943.
E-mail address: konstantin.efimov@pci.uni-hannover.de (K. Efimov).

0376-7388/$ – see front matter © 2011 Elsevier B.V. All rights reserved.
doi:10.1016/j.memsci.2011.10.030

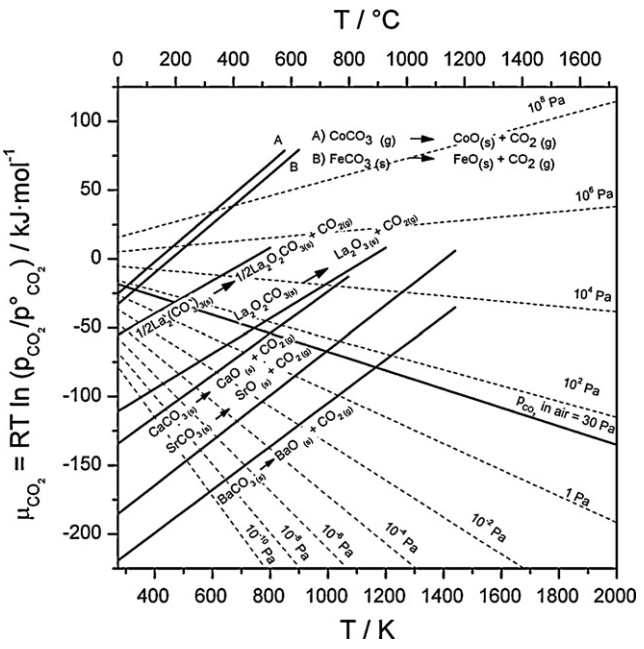

Fig. 1. Ellingham diagram for the decomposition of carbonates under different partial pressures. Chemical potential of CO_2 above $FeCO_3$, $CoCO_3$, $CaCO_3$, $La_2O_2CO_3$, $SrCO_3$, and $BaCO_3$ have been calculated from thermodynamic data [21–23]. The chemical potential of $La_2(CO_3)_3$ has been determined experimentally [24]. The dashed lines represent the chemical potential of CO_2 in the surrounding atmosphere for different partial pressures. $p^\circ(CO_2) = 101.3$ kPa refers to standard conditions.

[27,28]. Nevertheless, the desirable stability of Ca-containing materials in the presence of CO_2 can be expected from thermodynamic considerations and was reported for $Ca(Ti_{1-x}Fe_x)O_{3-\delta}$ [29].

Teraoka et al. have already reported a high oxygen permeation flux through the perovskite membrane with the composition $(La_{0.6}Ca_{0.4})(Co_{0.8}Fe_{0.2})O_{3-\delta}$ in 1988 [30]. Using a higher Ca content, Stevenson et al. have obtained a very high electrical conductivity using $(La_{0.4}Ca_{0.6})(Co_{0.8}Fe_{0.2})O_{3-\delta}$ perovskite in 1996 [31]. Since then, however, Ca-containing materials have gained little notice as promising MIEC materials [32–34]. One reason for this lack of attention may be the formation of secondary phases, like brownmillerite and/or the Grenier phase, during the preparation and operation of the perovskites. It has also been reported that this problem appears more pronounced with rising Ca content in the materials [31,35].

Recently, the group around Teraoka has developed asymmetrically structured membranes consisting of a porous support and thin dense layer and having the chemical composition $(La_{0.6}Ca_{0.4})CoO_{3-\delta}$ [36]. The main advantage of self-supported membranes is a result of the good chemical compatibility and thermomechanical stability of the materials. The oxygen permeation flux of the $(La_{0.6}Ca_{0.4})CoO_{3-\delta}$ was enhanced by the asymmetric configuration up to 300%, which has yielded a value of 1.66 $cm^3\ min^{-1}\ cm^{-2}$ [37]. This feature draws a spotlight on the Ca-containing perovskites as promising candidate MIEC materials.

In the present work, model perovskite systems $(La_{1-x}Ca_x)FeO_{3-\delta}$ and $(La_{1-x}Ca_x)(Co_{0.8}Fe_{0.2})O_{3-\delta}$ ($x = 0.4$–0.6) were examined regarding phase purity and stability in the presence of CO_2. Furthermore, bulk and asymmetrically structured membranes were prepared and investigated for their oxygen-ionic conducting properties.

2. Experimental

2.1. Powder preparation

A sol–gel route using metal nitrates, citric acid, and ethylenediaminetetraacetic acid (EDTA) was applied to prepare the $La_{1-x}Ca_xFeO_{3-\delta}$ and $La_{1-x}Ca_xCo_{0.8}Fe_{0.2}O_{3-\delta}$ ($x = 0.4$–0.6) materials as described elsewhere [38,39]. Given amounts of $La(NO_3)_3$ and $Ni(NO_3)_2$ were dissolved in water followed by the addition of EDTA as an organic ligand and citric acid as a network former. The molar ratio of metal nitrates:EDTA:citric acid was equal to 2:1:1.5. The pH value of the solution was adjusted to the range of 7–9 with $NH_3{\cdot}H_2O$. The transparent reaction solution was then heated at 423 K under constant stirring for several hours to obtain a gel. The gel was pre-calcined in the temperature range of 573–673 K in order to remove organic compounds, followed by calcination for 10 h at 1223 K in air.

2.2. Preparation of bulk and asymmetric membranes

To obtain the bulk membranes, the powders were uniaxially pressed under 140–150 kN for 20 min into green bodies. The pellets were then calcined for 10 h at 1423–1523 K with a heating and cooling rate of 3 K/min.

The asymmetric membranes were manufactured as follows: the as synthesized powders were ground in a mortar with 20 wt.% of a pore former block co-polymer Pluronic F 127 (BASF). The mixture was then press-formed into pellets and fired at 1423 K for 2 h. The dense layers were obtained by spin coating of porous supports with 3 cm^3 slurry (15 wt.% powder in ethanol), drying at room temperature for 5 h following by calcination at 1423–1523 K for 2–5 h.

2.3. Characterizations of materials

The phase structure of the powders and membranes were studied by X-ray diffraction (XRD, D8 Advance, Bruker-AXS, with Cu $K\alpha_{1,2}$ radiation). Data sets were recorded in a step–scan mode in the 2Θ range of 20–60° with intervals of 0.02°. *In situ* XRD tests were conducted in a high-temperature cell HTK 1200N (Anton-Paar) between room temperature and 1273 K. Tests in the atmosphere containing 50 vol.% CO_2/50 vol.% air and 50 vol.% CO_2/50 vol.% N_2 were carried out with heating and cooling rate of 12 °C/min. At each temperature step, the temperature was held for 30 min before diffraction data collection.

Scanning electron microscopy (SEM) imaging was performed on a JEOL JSM-6700F field-emission instrument at a low excitation voltage of 2 kV. An energy-dispersive X-ray spectrometer (EDXS), Oxford Instruments INCA-300, with an ultrathin window was used for the elemental analysis at an excitation voltage of 15 kV.

Transmission electron microscopy (TEM) investigations were made at 200 kV on a JEOL JEM-2100F-UHR field-emission instrument ($C_S = 0.5$ mm, $C_C = 1.2$ mm) equipped with a light-element EDXS detector (INCA 200 TEM, Oxford Instruments). The microscope was operated as scanning TEM (STEM) in high-angle annular dark-field (HAADF) mode. An energy filter of the type Gatan GIF 2001 was employed to acquire electron energy-loss spectra (EELS).

Specimens for electron microscopy were prepared as follow. First, the permeate side was glued with a polycrystalline corundum block using epoxy followed by cutting of membrane into 1 mm × 1 mm × 2 mm pieces. The protected membrane pieces were polished on polymer-embedded diamond lapping films to approximately 0.01 mm × 1 mm × 2 mm (Allied High Tech, Multiprep). Electron transparency for TEM was achieved by Ar^+ ion sputtering at 3 kV (Gatan, model 691 PIPS, precision ion polishing system) under shallow incident angles of 10°, 6°, and 4°.

Oxygen permeation was measured in a high-temperature permeation cell according to the method described elsewhere [40,41]. Before measurements, the bulk membranes were polished with 30 μm polymer-embedded diamond lapping films. Air was fed at a